

TOPICAL REVIEW

Applications of magnetic nanoparticles in biomedicine

Q A Pankhurst¹, J Connolly², S K Jones³ and J Dobson⁴

¹ Department of Physics and Astronomy, and London Centre for Nanotechnology, University College London, Gower Street, London WC1E 6BT, UK

² Department of Applied Physics, Curtin University of Technology, GPO Box U1987, Perth 6845, Western Australia

³ SIRTeX Medical Limited, PO Box 760, North Ryde, New South Wales 2113, Australia

⁴ Department of Biomedical Engineering and Medical Physics, Centre for Science and Technology in Medicine, Keele University, Stoke-on-Trent ST4 7QB, UK

E-mail: q.pankhurst@ucl.ac.uk

Received 4 April 2002

Published 18 June 2003

Online at stacks.iop.org/JPhysD/36/R167

Abstract

The physical principles underlying some current biomedical applications of magnetic nanoparticles are reviewed. Starting from well-known basic concepts, and drawing on examples from biology and biomedicine, the relevant physics of magnetic materials and their responses to applied magnetic fields are surveyed. The way these properties are controlled and used is illustrated with reference to (i) magnetic separation of labelled cells and other biological entities; (ii) therapeutic drug, gene and radionuclide delivery; (iii) radio frequency methods for the catabolism of tumours via hyperthermia; and (iv) contrast enhancement agents for magnetic resonance imaging applications. Future prospects are also discussed.

1. Introduction

Magnetic nanoparticles offer some attractive possibilities in biomedicine. First, they have controllable sizes ranging from a few nanometres up to tens of nanometres, which places them at dimensions that are smaller than or comparable to those of a cell (10–100 μm), a virus (20–450 nm), a protein (5–50 nm) or a gene (2 nm wide and 10–100 nm long). This means that they can ‘get close’ to a biological entity of interest. Indeed, they can be coated with biological molecules to make them interact with or bind to a biological entity, thereby providing a controllable means of ‘tagging’ or addressing it. Second, the nanoparticles are magnetic, which means that they obey Coulomb’s law, and can be manipulated by an external magnetic field gradient. This ‘action at a distance’, combined with the intrinsic penetrability of magnetic fields into human tissue, opens up many applications involving the transport and/or immobilization of magnetic nanoparticles, or of magnetically tagged biological entities. In this way they can be made to deliver a package, such as an anticancer drug, or a cohort of radionuclide atoms, to a targeted region of the

body, such as a tumour. Third, the magnetic nanoparticles can be made to resonantly respond to a time-varying magnetic field, with advantageous results related to the transfer of energy from the exciting field to the nanoparticle. For example, the particle can be made to heat up, which leads to their use as hyperthermia agents, delivering toxic amounts of thermal energy to targeted bodies such as tumours; or as chemotherapy and radiotherapy enhancement agents, where a moderate degree of tissue warming results in more effective malignant cell destruction. These, and many other potential applications, are made available in biomedicine as a result of the special physical properties of magnetic nanoparticles.

In this paper we will address the underlying physics of the biomedical applications of magnetic nanoparticles. After reviewing some of the relevant basic concepts of magnetism, including the classification of different magnetic materials and how a magnetic field can exert a force at a distance, we will consider four particular applications: magnetic separation, drug delivery, hyperthermia treatments and magnetic resonance imaging (MRI) contrast enhancement. We will conclude with an outlook on future prospects in this area,

especially with regard to the challenges faced in bringing current laboratory-tested technologies into mainstream use.

2. Basic concepts

2.1. $M-H$ curves

Figure 1 shows a schematic diagram of a blood vessel into which some magnetic nanoparticles have been injected. The magnetic properties of both the injected particles and the ambient biomolecules in the blood stream are illustrated by their different magnetic field response curves. To understand these curves better, we need to be aware of some of the fundamental concepts of magnetism, which will be recalled briefly here. Further details can be found in one of the many excellent textbooks on magnetism (e.g. [1, 2]).

If a magnetic material is placed in a magnetic field of strength H , the individual atomic moments in the material contribute to its overall response, the magnetic induction:

$$\mathbf{B} = \mu_0(\mathbf{H} + \mathbf{M}), \quad (1)$$

where μ_0 is the permeability of free space, and the magnetization $\mathbf{M} = \mathbf{m}/V$ is the magnetic moment per unit

volume, where \mathbf{m} is the magnetic moment on a volume V of the material. All materials are magnetic to some extent, with their response depending on their atomic structure and temperature. They may be conveniently classified in terms of their volumetric magnetic susceptibility, χ , where

$$\mathbf{M} = \chi\mathbf{H}, \quad (2)$$

describes the magnetization induced in a material by \mathbf{H} . In SI units χ is dimensionless and both \mathbf{M} and \mathbf{H} are expressed in A m^{-1} . Most materials display little magnetism, and even then only in the presence of an applied field; these are classified either as paramagnets, for which χ falls in the range 10^{-6} – 10^{-1} , or diamagnets, with χ in the range -10^{-6} to -10^{-3} . However, some materials exhibit ordered magnetic states and are magnetic even without a field applied; these are classified as ferromagnets, ferrimagnets and antiferromagnets, where the prefix refers to the nature of the coupling interaction between the electrons within the material [2]. This coupling can give rise to large spontaneous magnetizations; in ferromagnets \mathbf{M} is typically 10^4 times larger than would appear otherwise.

The susceptibility in ordered materials depends not just on temperature, but also on \mathbf{H} , which gives rise to the characteristic sigmoidal shape of the $M-H$ curve, with \mathbf{M} approaching a saturation value at large values of \mathbf{H} . Furthermore, in ferromagnetic and ferrimagnetic materials one often sees hysteresis, which is an irreversibility in the magnetization process that is related to the pinning of magnetic domain walls at impurities or grain boundaries within the material, as well as to intrinsic effects such as the magnetic anisotropy of the crystalline lattice. This gives rise to open $M-H$ curves, called hysteresis loops. The shape of these loops are determined in part by particle size: in large particles (of the order micron size or more) there is a multi-domain ground state which leads to a narrow hysteresis loop since it takes relatively little field energy to make the domain walls move; while in smaller particles there is a single domain ground state which leads to a broad hysteresis loop. At even smaller sizes (of the order of tens of nanometres or less) one can see superparamagnetism, where the magnetic moment of the particle as a whole is free to fluctuate in response to thermal energy, while the individual atomic moments maintain their ordered state relative to each other. This leads to the anhysteretic, but still sigmoidal, $M-H$ curve shown in figure 1.

The underlying physics of superparamagnetism is founded on an activation law for the relaxation time τ of the net magnetization of the particle [3, 4]:

$$\tau = \tau_0 \exp\left(\frac{\Delta E}{k_B T}\right), \quad (3)$$

where ΔE is the energy barrier to moment reversal, and $k_B T$ is the thermal energy. For non-interacting particles the pre-exponential factor τ_0 is of the order 10^{-10} – 10^{-12} s and only weakly dependent on temperature [4]. The energy barrier has several origins, including both intrinsic and extrinsic effects such as the magnetocrystalline and shape anisotropies, respectively; but in the simplest of cases it has a uniaxial form and is given by $\Delta E = KV$, where K is the anisotropy energy density and V is the particle

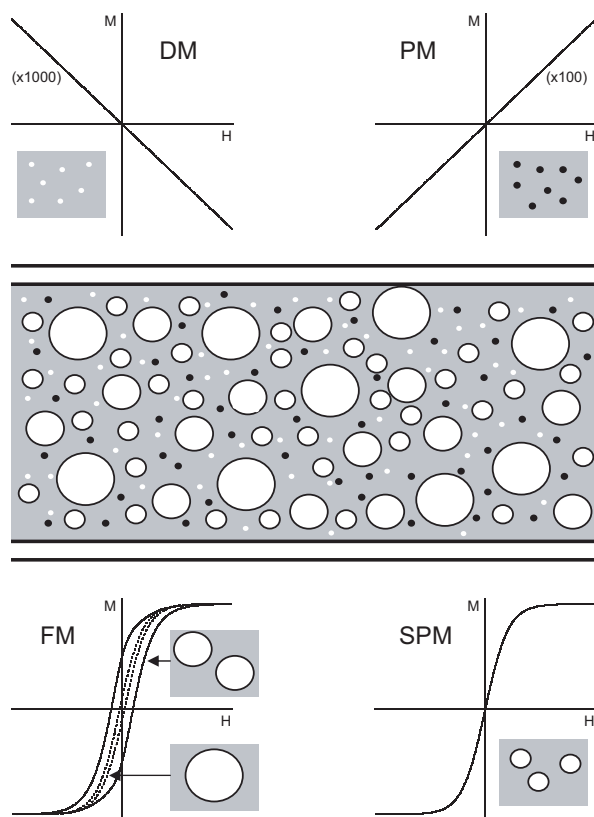


Figure 1. Magnetic responses associated with different classes of magnetic material, illustrated for a hypothetical situation in which ferromagnetic particles of a range of sizes from nanometre up to micron scale are injected into a blood vessel. $M-H$ curves are shown for diamagnetic (DM) and paramagnetic (PM) biomaterials in the blood vessel, and for the ferromagnetic (FM) injected particles, where the response can be either multi-domain (--- in FM diagram), single-domain (— in FM diagram) or superparamagnetic (SPM), depending on the size of the particle.

volume. This direct proportionality between ΔE and V is the reason that superparamagnetism—the thermally activated flipping of the net moment direction—is important for small particles, since for them ΔE is comparable to $k_B T$ at, say, room temperature. However, it is important to recognize that observations of superparamagnetism are implicitly dependent not just on temperature, but also on the measurement time τ_m of the experimental technique being used (see figure 2). If $\tau \ll \tau_m$ the flipping is fast relative to the experimental time window and the particles appear to be paramagnetic (PM); while if $\tau \gg \tau_m$ the flipping is slow and quasi-static properties are observed—the so-called ‘blocked’ state of the system. A ‘blocking temperature’ T_B is defined as the mid-point between these two states, where $\tau = \tau_m$. In typical experiments τ_m can range from the slow to medium timescales of 10^2 s for DC magnetization and 10^{-1} – 10^{-5} s for AC susceptibility, through to the fast timescales of 10^{-7} – 10^{-9} s for ^{57}Fe Mössbauer spectroscopy.

All of the different magnetic responses discussed above are illustrated in figure 1 for the case of ferromagnetic or ferrimagnetic nanoparticles injected into a blood vessel. Depending on the particle size, the injected material exhibits either a multi-domain, single-domain or superparamagnetic (SPM) M – H curve. The magnetic response of the blood vessel itself includes both a PM response—for example, from the iron-containing haemoglobin molecules, and a diamagnetic (DM) response—for example, from those intra-vessel proteins that comprise only carbon, hydrogen, nitrogen and oxygen atoms. It should be noted that the magnetic signal from the injected particles, whatever their size, far exceeds that from the blood vessel itself. This heightened selectivity is one of the advantageous features of biomedical applications of magnetic nanoparticles.

Returning to the hysteresis which gives rise to the open M – H curves seen for ferromagnets and antiferromagnets, it is clear that energy is needed to overcome the barrier to

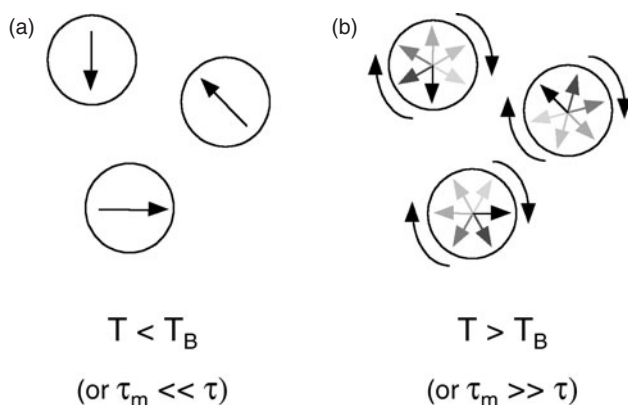


Figure 2. Illustration of the concept of superparamagnetism, where the circles depict three magnetic nanoparticles, and the arrows represent the net magnetization direction in those particles. In case (a), at temperatures well below the measurement-technique-dependent blocking temperature T_B of the particles, or for relaxation times τ (the time between moment reversals) much longer than the characteristic measurement time τ_m , the net moments are quasi-static. In case (b), at temperature well above T_B , or for τ much shorter than τ_m , the moment reversals are so rapid that in zero external field the time-averaged net moment on the particles is zero.

domain wall motion imposed by the intrinsic anisotropy and microstructural impurities and grain boundaries in the material. This energy is delivered by the applied field, and can be characterized by the area enclosed by the hysteresis loop. This leads to the concept that if one applies a time-varying magnetic field to a ferromagnetic or ferrimagnetic material, one can establish a situation in which there is a constant flow of energy into that material, which will perforce be transferred into thermal energy. This is the physical basis of hyperthermia treatments, which are discussed further in section 5. Note that a similar argument regarding energy transfer can be made for SPM materials, where the energy is needed to coherently align the particle moments to achieve the saturated state; this also is discussed in more detail in section 5.

2.2. Forces on magnetic nanoparticles

To understand how a magnetic field may be used to manipulate magnetic nanoparticles, we need to recall some elements of vector field theory. This is not always intuitive, and the reader is directed to recent reviews for further details [5–7]. It is also important to recognize that a magnetic field gradient is required to exert a force at a distance; a uniform field gives rise to a torque, but no translational action. We start from the definition of the magnetic force acting on a point-like magnetic dipole \mathbf{m} :

$$\mathbf{F}_m = (\mathbf{m} \cdot \nabla)\mathbf{B}, \quad (4)$$

which can be geometrically interpreted as differentiation with respect to the direction of \mathbf{m} . For example, if $\mathbf{m} = (0, 0, m_z)$ then $\mathbf{m} \cdot \nabla = m_z(\partial/\partial z)$ and a force will be experienced on the dipole provided there is a field gradient in \mathbf{B} in the z -direction. In the case of a magnetic nanoparticle suspended in a weakly DM medium such as water, the total moment on the particle can be written $\mathbf{m} = V_m \mathbf{M}$, where V_m is the volume of the particle and \mathbf{M} is its volumetric magnetization, which in turn is given by $\mathbf{M} = \Delta\chi \mathbf{H}$, where $\Delta\chi = \chi_m - \chi_w$ is the effective susceptibility of the particle relative to the water. For the case of a dilute suspension of nanoparticles in pure water, we can approximate the overall response of the particles plus water system by $\mathbf{B} = \mu_0 \mathbf{H}$, so that equation (4) becomes:

$$\mathbf{F}_m = \frac{V_m \Delta\chi}{\mu_0} (\mathbf{B} \cdot \nabla)\mathbf{B}. \quad (5)$$

Furthermore, provided there are no time-varying electric fields or currents in the medium, we can apply the Maxwell equation $\nabla \times \mathbf{B} = 0$ to the following mathematical identity:

$$\nabla(\mathbf{B} \cdot \mathbf{B}) = 2\mathbf{B} \times (\nabla \times \mathbf{B}) + 2(\mathbf{B} \cdot \nabla)\mathbf{B} = 2(\mathbf{B} \cdot \nabla)\mathbf{B}, \quad (6)$$

to obtain a more intuitive form of equation (5):

$$\mathbf{F}_m = V_m \Delta\chi \nabla \left(\frac{B^2}{2\mu_0} \right) \quad \text{or} \quad (7)$$

$$\mathbf{F}_m = V_m \Delta\chi \nabla \left(\frac{1}{2} \mathbf{B} \cdot \mathbf{H} \right),$$

in which the magnetic force is related to the differential of the magnetostatic field energy density, $\frac{1}{2} \mathbf{B} \cdot \mathbf{H}$. Thus, if $\Delta\chi > 0$ the magnetic force acts in the direction of steepest ascent of the energy density scalar field. This explains why, for example, when iron filings are brought near the pole of a permanent bar magnet, they are attracted towards that pole. It is also the basis for the biomedical applications of magnetic separation and drug delivery, as will be discussed in sections 3 and 4.

3. Magnetic separation

3.1. Cell labelling and magnetic separation

In biomedicine it is often advantageous to separate out specific biological entities from their native environment in order that concentrated samples may be prepared for subsequent analysis or other use. Magnetic separation using biocompatible nanoparticles is one way to achieve this. It is a two-step process, involving (i) the tagging or labelling of the desired biological entity with magnetic material, and (ii) the separating out of these tagged entities via a fluid-based magnetic separation device.

Tagging is made possible through chemical modification of the surface of the magnetic nanoparticles, usually by coating with biocompatible molecules such as dextran, polyvinyl alcohol (PVA) and phospholipids—all of which have been used on iron oxide nanoparticles [8–10]. As well as providing a link between the particle and the target site on a cell or molecule, coating has the advantage of increasing the colloidal stability of the magnetic fluid. Specific binding sites on the surface of cells are targeted by antibodies or other biological macromolecules such as hormones or folic acid [11–13]. As antibodies specifically bind to their matching antigen this provides a highly accurate way to label cells. For example, magnetic particles coated with immunospecific agents have been successfully bound to red blood cells [8, 14], lung cancer cells [15], bacteria [16], urological cancer cells [17] and Golgi vesicles [18]. For larger entities such as the cells, both magnetic nanoparticles and larger particles can be used: for example, some applications use magnetic ‘microspheres’—micron sized agglomerations of sub-micron sized magnetic particles incorporated in a polymeric binder [19].

The magnetically labelled material is separated from its native solution by passing the fluid mixture through a region in which there is a magnetic field gradient which can immobilize the tagged material via the magnetic force of equation (7). This force needs to overcome the hydrodynamic drag force acting on the magnetic particle in the flowing solution,

$$F_d = 6\pi\eta R_m \Delta v, \quad (8)$$

where η is the viscosity of the medium surrounding the cell (e.g. water), R_m is the radius of the magnetic particle, and $\Delta v = v_m - v_w$ is the difference in velocities of the cell and the water [6]. There is also buoyancy force that affects the motion, but this is dependent on the difference between the density of the cell and the water, and for most cases of interest in biology and medicine can be neglected. Equating the hydrodynamic drag and magnetic forces, and writing $V_m = \frac{4}{3}\pi R_m^3$, gives the velocity of the particle relative to the carrier fluid as:

$$\Delta v = \frac{R_m^2 \Delta \chi}{9\mu_0 \eta} \nabla(B^2) \quad \text{or} \quad \Delta v = \frac{\xi}{\mu_0} \nabla(B^2), \quad (9)$$

where ξ is the ‘magnetophoretic mobility’ of the particle—a parameter that describes how manipulable a magnetic particle is. For example, the magnetophoretic mobility of magnetic microspheres can be much greater than that of nanoparticles, due to their larger size. This can be an advantage, for example, in cell separations, where the experimental timeframe for the separations is correspondingly shorter. On the other hand,

smaller magnetic particle sizes can also be advantageous, for example, in reducing the likelihood that the magnetic material will interfere with further tests on the separated cells [20].

3.2. Separator design

Magnetic separator design can be as simple as the application and removal of a permanent magnet to the wall of a test tube to cause aggregation, followed by removal of the supernatant (figure 3(a)). However, this method can be limited by slow accumulation rates [21]. It is often preferable to increase the separator efficiency by producing regions of high magnetic field gradient to capture the magnetic nanoparticles as they float or flow by in their carrier medium. A typical way to achieve this is to loosely pack a flow column with a magnetizable matrix of wire (e.g. steel wool) or beads [22] and to pump the magnetically tagged fluid through the column while a field is applied (figure 3(b)). This method is faster than in the first case, although problems can arise due to the settling and adsorption of magnetically tagged material on the matrix. An alternative, rapid throughput method which does not involve any obstructions being placed in the column is the use of specifically designed field gradient systems, such as the quadrupolar arrangement shown in figure 4 which creates a magnetic gradient radially outwards from the centre of the flow column [23].

As well as separating out the magnetically tagged material, the spatially varying magnitude of the field gradient can be used to achieve ‘fluid flow fractionation’ [24]. This is a process in which the fluid is split at the outlet into fractions containing tagged cells or proteins with differing

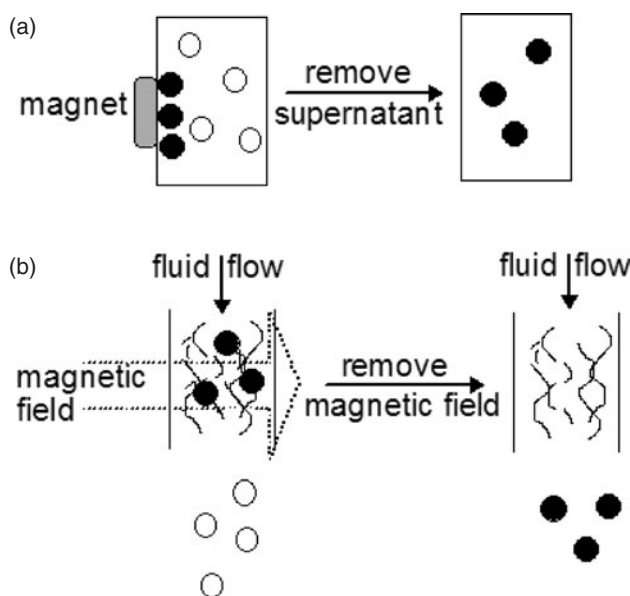


Figure 3. The standard methods of magnetic separation: in (a) a magnet is attached to the container wall of a solution of magnetically tagged (●) and unwanted (○) biomaterials. The tagged particles are gathered by the magnet, and the unwanted supernatant solution is removed. In (b) a solution containing tagged and unwanted biomaterials flows continuously through a region of strong magnetic field gradient, often provided by packing the column with steel wool, which captures the tagged particles. Thereafter the tagged particles are recovered by removing the field and flushing through with water.

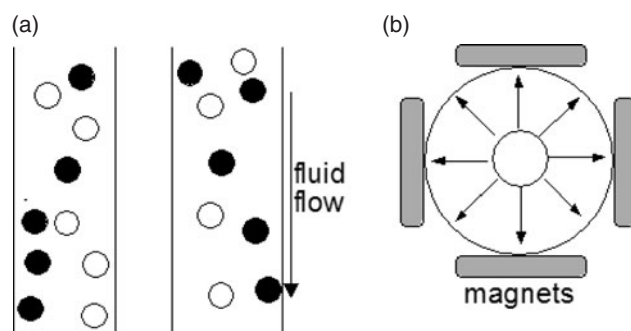


Figure 4. A rapid throughput method of magnetic separation, in which an annular column containing a flowing solution of magnetically tagged (●) and unwanted (○) biomaterials is placed within a set of magnets arranged in quadrature: (a) longitudinal cross-section of the annular column; (b) transverse cross-section of the four magnets with the resulting magnetic field lines. Under the action of the magnetic field gradient the tagged particles move to the column walls, where they are held until the field is removed and they are recovered by flushing through with water. The central core of the column is made of non-magnetic material to avoid complications due to the near-zero field gradients there.

magnetophoretic mobilities. In a variant of this, the fluid is static while an applied magnetic field is moved up the container [25]. The particles move up the container in the resulting field gradient at a velocity dependent on their magnetophoretic mobility. At the top of the container they enter a removable section and are held here by a permanent magnet. The bottom section of the container moves to the next section, a magnetic field with different strength to the first is applied and the process repeats. The result is a fractionation of the sample into aliquots of differing magnetophoretic mobility.

3.3. Applications

Magnetic separation has been successfully applied to many aspects of biomedical and biological research. It has proven to be a highly sensitive technique for the selection of rare tumour cells from blood, and is especially well suited to the separation of low numbers of target cells [26]. This has, for example, led to the enhanced detection of malarial parasites in blood samples either by utilizing the magnetic properties of the parasite [27] or through labelling the red blood cells with an immunospecific magnetic fluid [28]. It has been used as a pre-processing technology for polymerase chain reactions, through which the DNA of a sample is amplified and identified [29]. Cell counting techniques have also been developed. One method estimates the location and number of cells tagged by measuring the magnetic moment of the microsphere tags [30], while another uses a giant magnetoresistive sensor to measure the location of microspheres attached to a surface layered with a bound analyte [31].

In another application, magnetic separation has been used in combination with optical sensing to perform ‘magnetic enzyme linked immunosorbent assays’ [32, 33]. These assays use fluorescent enzymes to optically determine the number of cells labelled by the assay enzymes. Typically the target material must first be bound to a solid matrix. In a modification of this procedure the magnetic microspheres act as the surface for initial immobilization of the target material and magnetic

separation is used to increase the concentration of the material. The mobility of the magnetic nanoparticles allows a shorter reaction time and a greater volume of reagent to be used than in standard immunoassays where the antibody is bound to a plate. In a variation of this procedure, magnetic separation has been used to localize labelled cells at known locations for cell detection and counting via optical scanning [14]. The cells are labelled both magnetically and fluorescently and move through a magnetic field gradient towards a plate on which lines of ferromagnetic material have been lithographically etched. The cells align along these lines and the fluorescent tag is used for optical detection of the cells.

4. Drug delivery

4.1. Motivation and physical principles

The major disadvantage of most chemotherapies is that they are relatively non-specific. The therapeutic drugs are administered intravenously leading to general systemic distribution, resulting in deleterious side-effects as the drug attacks normal, healthy cells in addition to the target tumour cells. For example, the side effects of anti-inflammatory drugs on patients who have chronic arthritis can lead to the discontinuation of their use. However, if such treatments could be localized, e.g. to the site of a joint, then the continued use of these very potent and effective agents could be made possible.

Recognition of this led researchers in the late 1970s to propose the use of magnetic carriers to target specific sites (generally cancerous tumours) within the body [34–36]. The objectives are two-fold: (i) to reduce the amount of systemic distribution of the cytotoxic drug, thus reducing the associated side-effects; and (ii) to reduce the dosage required by more efficient, localized targeting of the drug. In magnetically targeted therapy, a cytotoxic drug is attached to a biocompatible magnetic nanoparticle carrier. These drug/carrier complexes—usually in the form of a biocompatible ferrofluid—are injected into the patient via the circulatory system. When the particles have entered the bloodstream, external, high-gradient magnetic fields are used to concentrate the complex at a specific target site within the body (figure 5). Once the drug/carrier is concentrated at the target, the drug can be released either via enzymatic activity or changes in physiological conditions such as pH, osmolality, or temperature [37], and be taken up by the tumour cells. This system, in theory, has major advantages over the normal, non-targeted methods of cytotoxic drug therapy.

The physical principles underlying magnetic targeting therapy are similar to those used in magnetic separation, and are derived from the magnetic force exerted on a SPM nanoparticle by a magnetic field gradient, as in equation (7). The effectiveness of the therapy is dependent on several physical parameters, including the field strength, gradient and volumetric and magnetic properties of the particles. As the carriers (ferrofluids) are normally administered intravenously or intra-arterially, hydrodynamic parameters such as blood flow rate, ferrofluid concentration, infusion route and circulation time also will play a major role—as will physiological parameters such as tissue depth to the target site (i.e. distance from the magnetic field source), reversibility and strength of the drug/carrier binding, and tumour volume [38].

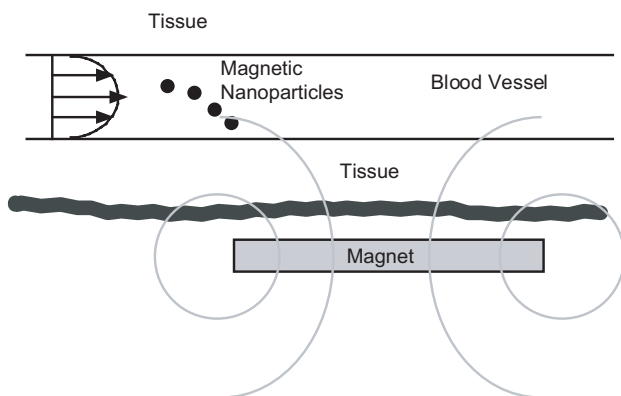


Figure 5. A hypothetical magnetic drug delivery system shown in cross-section: a magnet is placed outside the body in order that its magnetic field gradient might capture magnetic carriers flowing in the circulatory system.

In general, larger particles (e.g. magnetic microspheres, ca $1\ \mu\text{m}$ in diameter, comprising agglomerates of SPM particles) are more effective at withstanding flow dynamics within the circulatory system—particularly in larger veins and arteries. In most cases the magnetic field gradient is generated by a strong permanent magnet, such as Nd-Fe-B, fixed outside the body over the target site. Preliminary investigations of the hydrodynamics of drug targeting suggest that for most magnetite-based carriers, flux densities at the target site must be of the order of $0.2\ \text{T}$ with field gradients of approximately $8\ \text{T m}^{-1}$ for femoral arteries and greater than $100\ \text{T m}^{-1}$ for carotid arteries [39]. This suggests that targeting is likely to be most effective in regions of slower blood flow, particularly if the target site is closer to the magnet source. More recently, Richardson and others have developed mathematical models to determine particle trajectories for a variety of field/particle configurations in two dimensions, including consideration of their motion as they approach the vessel wall [40]. This is significant since near the walls the particle motion is no longer governed by Stoke's law for the drag force, equation (8), and the hydrodynamic parameters are modified. Experimental work is underway to inform the development of such models [41].

4.2. Magnetic drug carriers

Since the first magnetic polymer carriers of the 1970s, a variety of magnetic nanoparticle and microparticle carriers have been developed to deliver drugs to specific target sites *in vivo*. The optimization of these carriers continues today. Generally, the magnetic component of the particle is coated by a biocompatible polymer such as PVA or dextran, although recently inorganic coatings such as silica have been developed. The coating acts to shield the magnetic particle from the surrounding environment and can also be functionalized by attaching carboxyl groups, biotin, avidin, carbodi-imide and other molecules [42–44]. As shown in figure 6, these molecules then act as attachment points for the coupling of cytotoxic drugs or target antibodies to the carrier complex.

The carriers typically have one of two structural configurations: (i) a magnetic particle core (usually magnetite, Fe_3O_4 , or maghemite, $\gamma\text{-Fe}_2\text{O}_3$) coated with a biocompatible

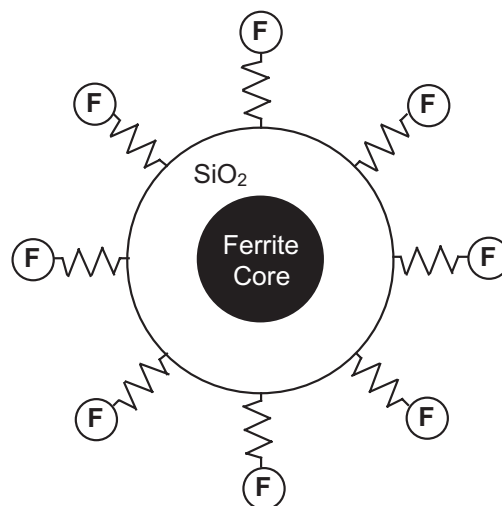


Figure 6. Schematic diagram of a functionalized magnetic nanoparticle showing a core/shell structure with a shell of silica, SiO_2 , and functional groups attached to the shell.

polymer or (ii) a porous biocompatible polymer in which magnetic nanoparticles are precipitated inside the pores [45]. Recent developmental work on carriers has largely focused on new polymeric or inorganic coatings on magnetite/maghemite nanoparticles [10, 46–52], although noble metal coatings such as gold are also being considered [53]. Research also continues into alternative magnetic particles, such as iron, cobalt or nickel [54–56] or yttrium aluminium iron garnet [57]. Cobalt/silica carriers are currently being investigated for their use in eye surgery to repair detached retinas [58, 59].

4.3. Targeting studies

Magnetic carriers were first used to target cytotoxic drugs (doxorubicin) to sarcoma tumours implanted in rat tails [60]. The initial results were encouraging, showing a total remission of the sarcomas compared to no remission in another group of rats which were administered with ten times the dose but without magnetic targeting. Since that study, success in cytotoxic drug delivery and tumour remission has been reported by several groups using animal models including swine [61, 62], rabbits [37] and rats [38, 63, 64]. Kubo *et al* recently offered a variation on these techniques. They implanted permanent magnets at solid osteosarcoma sites in hamsters and delivered the cytotoxic compounds via magnetic liposomes. They reported a four-fold increase in cytotoxic drug delivery to the osteosarcoma sites when compared with normal intravenous (non-magnetic) delivery [65], as well as a significant increase in anti-tumour activity and the elimination of weight-loss as a side effect [66].

This technique has also been employed to target cytotoxic drugs to brain tumours. Brain tumours are particularly difficult targets due to the fact that the drug must cross the blood–brain barrier. Pulfer and Gallo [63] demonstrated that particles as large as $1\text{--}2\ \mu\text{m}$ could be concentrated at the site of intracerebral rat glioma-2 (RG-2) tumours. Though the concentration of the particles in the tumour was low, it was significantly higher than non-magnetic particles. In a later

study the group demonstrated that 10–20 nm magnetic particles were even more effective at targeting these tumours in rats [64]. Electron microscopic analysis of brain tissue samples revealed the presence of magnetic carriers in the interstitial space in tumours but in normal brain tissue, they were only found in the vasculature. Mykhaylyk and others [67] recently had less success using magnetite–dextran nanoparticles but were able to target rat glial tumours by disrupting the blood–brain barrier immediately prior to particle injection.

Studies of magnetic targeting in humans were rare up to now. A Phase I clinical trial conducted by Lübke and others [68–70] demonstrated that the infusion of ferrofluids was well tolerated in most of the 14 patients studied. In addition, the authors reported that the ferrofluid was successfully directed to the advanced sarcomas without associated organ toxicity. More recently, FeRx Inc. was granted fast-track status to proceed with multi-centre Phases I and II clinical trials of their magnetic targeting system for hepatocellular carcinomas (a type of liver tumour). This appears to be the most promising clinical application at present.

As promising as these results have been, there are several problems associated with magnetically targeted drug delivery [38, 71]. These limitations include (i) the possibility of embolization of the blood vessels in the target region due to accumulation of the magnetic carriers, (ii) difficulties in scaling up from animal models due to the larger distances between the target site and the magnet, (iii) once the drug is released, it is no longer attracted to the magnetic field, and (iv) toxic responses to the magnetic carriers. Recent pre-clinical and experimental results indicate, however, that it is still possible to overcome these limitations and use magnetic targeting to improve drug retention and also address safety issues [68, 72].

4.4. Radionuclide and gene delivery

One way to overcome the limitation caused by the release of the drug from the carrier is to use a system in which the therapeutic agent remains coupled to the magnetic carrier throughout the duration of the treatment. Based on this idea, the possibility of targeting radionuclides via magnetic carriers has been investigated. The advantage these complexes have over cytotoxic drug/magnetic carrier complexes is that the effectiveness of the radionuclide does not require the tumour cells to actually take up the agent. If the radionuclide is targeted to a region near the tumour site and held there, the radiation will affect the surrounding tumour tissue while it is still attached to the magnetic carrier. This type of system was tested in 1995 using *in vitro* and mouse models. In both cases, targeting of a magnetic carrier coupled to a β -emitter (Y-90) was effective at concentrating radiation to the desired site. In the mouse tumour model, there was a significant increase in radioactivity at the tumour site compared to using the same complex without a magnetic field: $73 \pm 32\%$ vs $6 \pm 4\%$ [73]. Since this study, Häfeli and others [74–76] have demonstrated the effectiveness of this technique in both animal and cell culture studies using both yttrium-90 and rhenium-188.

Investigations also have begun with a view towards using magnetic carriers for gene therapy. In this case, a viral vector carrying the therapeutic gene is coated onto the magnetic carrier's surface. By holding the carrier at the target site via

external magnetic fields, the virus is in contact with the tissue for a longer period of time, increasing the efficiency of gene transfection and expression [77, 78]. New magnetic carriers are being developed specifically for these applications [79] and this is an area which shows great promise.

5. Hyperthermia

5.1. Catabolism of tumours by hyperthermia

The possibility of treating cancer by artificially induced hyperthermia has led to the development of many different devices designed to heat malignant cells while sparing surrounding healthy tissue [80–82]. Experimental investigations of the application of magnetic materials for hyperthermia date back to 1957 when Gilchrist *et al* [83] heated various tissue samples with 20–100 nm size particles of γ -Fe₂O₃ exposed to a 1.2 MHz magnetic field. Since then there have been numerous publications describing a variety of schemes using different types of magnetic materials, different field strengths and frequencies and different methods of encapsulation and delivery of the particles [84–102]. In broad terms, the procedure involves dispersing magnetic particles throughout the target tissue, and then applying an AC magnetic field of sufficient strength and frequency to cause the particles to heat. This heat conducts into the immediately surrounding diseased tissue whereby, if the temperature can be maintained above the therapeutic threshold of 42°C for 30 min or more, the cancer is destroyed. Whereas the majority of hyperthermia devices are restricted in their utility because of unacceptable coincidental heating of healthy tissue, magnetic particle hyperthermia is appealing because it offers a way to ensure only the intended target tissue is heated (see figure 7).

5.2. Operational constraints

A number of studies have demonstrated the therapeutic efficacy of this form of treatment in animal models (see, e.g. the review

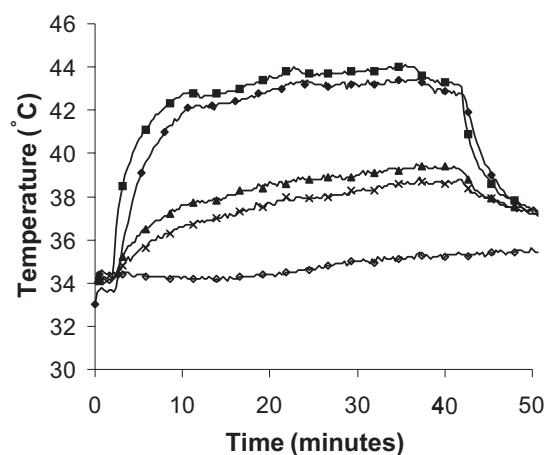


Figure 7. Animal trial data on hyperthermia treatments in rabbits, showing preferential heating of a tumour using intra-vascularly infused ferromagnetic microspheres: (■) tumour edge, (◆) tumour centre, (▲) normal liver 1–2 cm from tumour, (×) alternative lobe, and (◇) core body temperature.

by Moroz *et al* [103]). To date, however, there have been no reports of the successful application of this technology to the treatment of a human patient. The challenge lies in being able to deliver an adequate quantity of the magnetic particles to generate enough heat in the target using AC magnetic field conditions that are clinically acceptable. Most of the laboratory and animal model based studies reported so far are characterized by the use of magnetic field conditions that could not be safely used with a human patient. In most instances, reducing the field strength or frequency to safer levels would almost certainly lead to such a reduction in the heat output from the magnetic material as to render it useless in this application.

It is important therefore to understand the underlying physical mechanisms by which heat is generated in small magnetic particles by alternating magnetic fields. Enough heat must be generated by the particles to sustain tissue temperatures of at least 42°C for 30 min or so. Calculating the heat deposition rate required to achieve this is complicated by the presence of blood flow and tissue perfusion, both of which are dominant sources of tissue cooling and both of which vary actively as tissue is heated. Several authors have analysed the heat transfer problem whereby a defined volume of tissue is heated from within by evenly dispersed sources such as microscopic magnetic particles [104–106]. The problem posed by the cooling from discrete blood vessels is generally avoided because of the mathematical complexity and lack of generality of the results. However, an often-used rule of thumb is that a heat deposition rate of 100 mW cm⁻³ of tissue will suffice in most circumstances.

The frequency and strength of the externally applied AC magnetic field used to generate the heating is limited by deleterious physiological responses to high frequency magnetic fields [107, 108]. These include stimulation of peripheral and skeletal muscles, possible cardiac stimulation and arrhythmia, and non-specific inductive heating of tissue. Generally, the useable range of frequencies and amplitudes is considered to be $f = 0.05\text{--}1.2$ MHz and $H = 0\text{--}15$ kA m⁻¹. Experimental data on exposure to much higher frequency fields comes from groups such as Oleson *et al* [109] who developed a hyperthermia system based on inductive heating of tissue, and Atkinson *et al* [110] who developed a treatment system based on eddy current heating of implantable metal thermoseeds. Atkinson *et al* concluded that exposure to fields where the product $H \cdot f$ does not exceed 4.85×10^8 A m⁻¹ s⁻¹ is safe and tolerable.

The amount of magnetic material required to produce the required temperatures depends to a large extent on the method of administration. For example, direct injection allows for substantially greater quantities of material to be localized in a tumour than do methods employing intravascular administration or antibody targeting, although the latter two may have other advantages. A reasonable assumption is that ca 5–10 mg of magnetic material concentrated in each cm³ of tumour tissue is appropriate for magnetic hyperthermia in human patients.

Regarding the choice of magnetic particle, the iron oxides magnetite (Fe₃O₄) and maghemite (γ -Fe₂O₃) are the most studied to date because of their generally appropriate magnetic properties and biological compatibility, although many others

have been investigated. Particle sizes less than about 10 μ m are normally considered small enough to enable effective delivery to the site of the cancer, either via encapsulation in a larger moiety or suspension in some sort of carrier fluid. Nanoscale particles can be coupled with antibodies to facilitate targeting on an individual cell basis. Candidate materials are divided into two main classes; ferromagnetic or ferrimagnetic (FM) single domain or multi-domain particles, or SPM particles. The heat generating mechanisms associated with each class are quite different, each offering unique advantages and disadvantages, as discussed later.

5.3. Heating mechanisms

FM particles possess hysteretic properties when exposed to a time varying magnetic field, which gives rise to magnetically induced heating. The amount of heat generated per unit volume is given by the frequency multiplied by the area of the hysteresis loop:

$$P_{\text{FM}} = \mu_0 f \oint H dM. \quad (10)$$

This formula ignores other possible mechanisms for magnetically induced heating such as eddy current heating and ferromagnetic resonance, but these are generally irrelevant in the present context. The particles used for magnetic hyperthermia are much too small and the AC field frequencies much too low for the generation of any substantial eddy currents. Ferromagnetic resonance effects may become relevant but only at frequencies far in excess of those generally considered appropriate for this type of hyperthermia.

For FM particles well above the SPM size limit there is no implicit frequency dependence in the integral of equation (10), so P_{FM} can be readily determined from quasi-static measurements of the hysteresis loop using, for example, a VSM or SQUID magnetometer. As discussed in section 2, the re-orientation and growth of spontaneously magnetized domains within a given FM particle depends on both microstructural features such as vacancies, impurities or grain boundaries, and intrinsic features such as the magnetocrystalline anisotropy as well as the shape and size of the particle. In most cases it is not possible to predict *a priori* what the hysteresis loop will look like.

In principle, substantial hysteresis heating of the FM particles could be obtained using strongly anisotropic magnets such as Nd-Fe-B or Sm-Co; however, the constraints on the amplitude of H that can be used mean that fully saturated loops cannot be used. Minor (unsaturated) loops could be used, and would give rise to heating, but only at much reduced levels. In fact, as is evident in equation (10), the maximum realizable P_{FM} should involve a rectangular hysteresis loop. However, this could only be achieved with an ensemble of uniaxial particles perfectly aligned with H , a configuration that would be difficult if not impossible to achieve *in vivo*. For a more realistic ensemble of randomly aligned FM particles the most that can be hoped for is around 25% of this ideal maximum.

However, over the last decade the field of magnetic particle hyperthermia has been revitalized by the advent of ‘magnetic fluid hyperthermia’, where the magnetic entities are SPM

nanoparticles suspended in water or a hydrocarbon fluid to make a ‘magnetic fluid’ or ‘ferrofluid’ [98, 111, 112]. When a ferrofluid is removed from a magnetic field its magnetization relaxes back to zero due to the ambient thermal energy of its environment. This relaxation can correspond either to the physical rotation of the particles themselves within the fluid, or rotation of the atomic magnetic moments within each particle. Rotation of the particles is referred to as ‘Brownian rotation’ while rotation of the moment within each particle is known as ‘Néel relaxation’. Each of these processes is characterized by a relaxation time: τ_B for the Brownian process depends on the hydrodynamic properties of the fluid; while τ_N for the Néel process is determined by the magnetic anisotropy energy of the SPM particles relative to the thermal energy. Both Brownian and Néel processes may be present in a ferrofluid, whereas only τ_N is relevant in fixed SPM particles where no physical rotation of the particle is possible. The relaxation times τ_B and τ_N depend differently on particle size; losses due to Brownian rotation are generally maximized at a lower frequency than are those due to Néel relaxation for a given size.

The physical basis of the heating of SPM particles by AC magnetic fields has been reviewed by Rosensweig [113]. It is based on the Debye model, which was originally developed to describe the dielectric dispersion in polar fluids [114], and the recognition that the finite rate of change of M in a ferrofluid means that it will lag behind H . For small field amplitudes, and assuming minimal interactions between the constituent SPM particles, the response of the magnetization of a ferrofluid to an AC field can be described in terms of its complex susceptibility $\chi = \chi' + i\chi''$, where both χ' and χ'' are frequency dependent. The out-of-phase χ'' component results in heat generation given by [113]:

$$P_{\text{SPM}} = \mu_0 \pi f \chi'' H^2, \quad (11)$$

which can be interpreted physically as meaning that if M lags H there is a positive conversion of magnetic energy into internal energy. This simple theory compares favourably with experimental results, for example, in predicting a square dependence of P_{SPM} on H [91], and the dependence of χ'' on the driving frequency [115–117].

Measurements of the heat generation from magnetic particles are usually quoted in terms of the specific absorption rate (SAR) in units of W g^{-1} . Multiplying the SAR by the density of the particle yields P_{FM} and P_{SPM} , so the parameter allows comparison of the efficacies of magnetic particles covering all the size ranges [88, 111, 118–121]. It is clear from such comparisons that most real FM materials require applied field strengths of ca 100 kA m^{-1} or more before they approach a fully saturated loop, and therefore only minor hysteresis loops can be utilized given the operational constraint of ca 15 kA m^{-1} , giving rise to low SARs. In contrast, SPM materials are capable of generating impressive levels of heating at lower fields. For example, the best of the ferrofluids reported by Hergt *et al* [121] has a SAR of 45 W g^{-1} at 6.5 kA m^{-1} and 300 kHz which extrapolates to 209 W g^{-1} for 14 kA m^{-1} , compared to 75 W g^{-1} at 14 kA m^{-1} for the best FM magnetite sample. While all of these samples would be adequate for magnetic particle hyperthermia, importantly, it seems clear that ferrofluids and SPM particles are more likely to offer useful heating using lower magnetic field strengths.

6. MRI contrast enhancement

6.1. Physical principles

MRI relies on the counterbalance between the exceedingly small magnetic moment on a proton, and the exceedingly large number of protons present in biological tissue, which leads to a measurable effect in the presence of large magnetic fields [122, 123]. Thus, even though the effect of a steady state field of $B_0 = 1 \text{ T}$ on a collection of protons, such as the hydrogen nuclei in a water molecule, is so small that it is equivalent to only three of every million proton moments m being aligned parallel to B_0 , there are so many protons available— 6.6×10^{19} in every mm^3 of water—that the effective signal, 2×10^{14} proton moments per mm^3 , is observable. As illustrated in figure 8, this signal can be captured by making use of resonant absorption: applying a time-varying magnetic field in a plane perpendicular to B_0 , tuned to the Larmor precession frequency $\omega_0 = \gamma B_0$ of the protons. For ^1H protons the gyromagnetic ratio $\gamma = 2.67 \times 10^8 \text{ rad s}^{-1} \text{ T}^{-1}$, so that in a field of $B_0 = 1 \text{ T}$ the Larmor precession frequency corresponds to a radio frequency field with $\omega_0/2\pi = 42.57 \text{ MHz}$. In practice the radio frequency transverse field is applied in a pulsed sequence, of duration sufficient to derive a coherent response from the net magnetic moment of the protons in the MRI scanner. From the instant that the radio frequency pulse is turned off the relaxation of the coherent response is measured via induced currents in pick-up coils in the scanner. These resonantly tuned detection coils enhance the signal by a quality factor of ca 50–100. As shown in figure 8, for B_0 parallel to

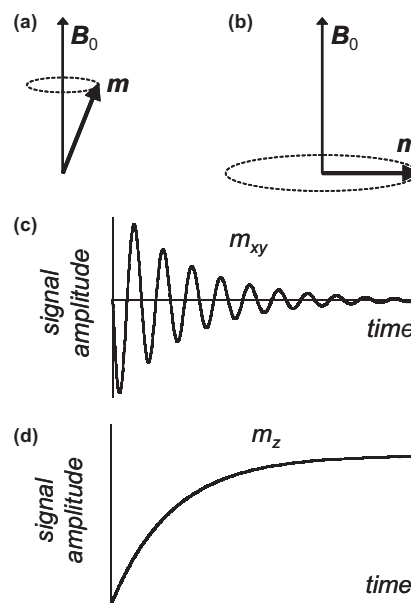


Figure 8. Illustration of magnetic resonance for a large ensemble of protons with net magnetic moment m in the presence of an external magnetic field B_0 . In (a) the net moment precesses around B_0 at the characteristic Larmor frequency, ω_0 . In (b) a second external field is applied, perpendicular to B_0 , oscillating at ω_0 . Despite being much weaker than B_0 , this has the effect of resonantly exciting the moment precession into the plane perpendicular to B_0 . In (c) and (d) the oscillating field is removed at time zero, and the in-plane (c) and longitudinal (d) moment amplitudes relax back to their initial values.

the z -axis these relaxation signals are of the form:

$$m_z = m(1 - e^{-t/T_1}) \quad (12)$$

and

$$m_{x,y} = m \sin(\omega_0 t + \phi) e^{-t/T_2}, \quad (13)$$

where T_1 and T_2 are the longitudinal (or spin–lattice) and transverse (or spin–spin) relaxation times, respectively, and ϕ is a phase constant. The longitudinal relaxation reflects a loss of energy, as heat, from the system to its surrounding ‘lattice’, and is primarily a measure of the dipolar coupling of the proton moments to their surroundings. The relaxation in the xy -plane is relatively rapid, and is driven by the loss of phase coherence in the precessing protons due to their magnetic interactions with each other and with other fluctuating moments in the tissue. Dephasing can also be affected by local inhomogeneities in the applied longitudinal field, leading to the replacement of T_2 in equation (13) by the shorter relaxation time, T_2^* :

$$\frac{1}{T_2^*} = \frac{1}{T_2} + \gamma \frac{\Delta B_0}{2}, \quad (14)$$

where ΔB_0 is the variation in the field brought about either through distortions in the homogeneity of the applied field itself, or by local variations in the magnetic susceptibility of the system [124, 125].

6.2. MRI contrast enhancement studies

Both T_1 and T_2^* can be shortened by the use of a magnetic contrast agent. The most common contrast agents currently used are PM gadolinium ion complexes, although agents based on SPM nanoparticles are commercially available, such as ‘Feridex I. V.’, an iron oxide contrast agent marketed by Advanced Magnetics Inc. for the organ-specific targeting of liver lesions. The SPM particles used are magnetically saturated in the normal range of magnetic field strengths used in MRI scanners, thereby establishing a substantial locally perturbing dipolar field which leads, via equation (14), to a marked shortening of T_2^* (see figure 9) along with a less marked reduction of T_1 [123].

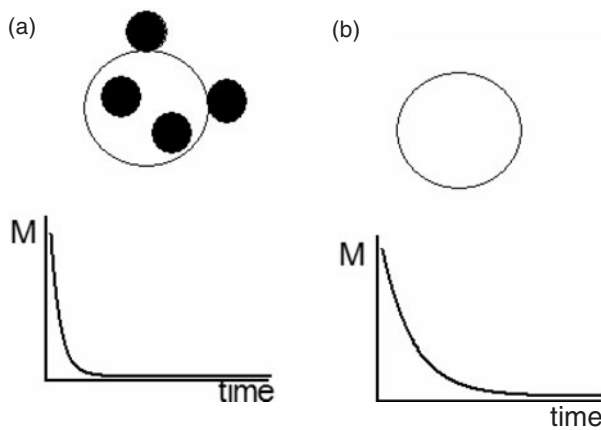


Figure 9. Effect of magnetic particle internalization in cells on T_2^* relaxation times: (a) the protons in cells tagged by magnetic particles have a shorter T_2^* relaxation time than those in (b) untagged cells.

Iron oxide nanoparticles are the most commonly used SPM contrast agents. Dextran coated iron oxides are biocompatible and are excreted via the liver after the treatment. They are selectively taken up by the reticuloendothelial system, a network of cells lining blood vessels whose function is to remove foreign substances from the bloodstream; MRI contrast relies on the differential uptake of different tissues [126]. There is also a size effect: nanoparticles with diameters of ca 30 nm or more are rapidly collected by the liver and spleen, while particles with sizes of ca 10 nm or less are not so easily recognized. The smaller particles therefore have a longer half-life in the blood stream and are collected by reticuloendothelial cells throughout the body, including those in the lymph nodes and bone marrow [127, 128]. Similarly, such agents have been used to visualize the vascular system [129], and to image the central nervous system [130]. It is also notable that tumour cells do not have the effective reticuloendothelial system of healthy cells, so that their relaxation times are not altered by the contrast agents. This has been used, for example, to assist the identification of malignant lymph nodes [131], liver tumours [132] and brain tumours [133].

Iron oxide nanoparticles also lend themselves to encapsulation into target-specific agents, such as a liposome that is known to localize in the bone marrow [134]. Dendrimer coatings comprising a highly branched polymer structure that has a high rate of non-cell-specific binding and intracellular uptake have also been used to good effect [135], as has the use of lipofection agents, normally used to carry DNA into the cell nucleus, to enable intracellular incorporation of the magnetic nanoparticles into stem cells [136]. Magnetic nanoparticles have also been utilized for the *in vivo* monitoring of gene expression, a process in which cells are engineered to over-express a given gene. This process leads to the production of increased numbers of certain cell wall receptors, which in turn can be targeted using specially coated nanoparticles, thereby allowing a differentiation between the expressing cells and their surroundings [137]. Another aspect of the targeting of cell receptors has been to selectively study cells that are in the process of cell death [138].

7. Discussion and future prospects

In this paper we have reviewed some basic concepts regarding the interactions between magnetic nanoparticles and a static or time-varying external magnetic field, and shown how these pertain to current biomedical applications of magnetic nanoparticles. We have focused in particular on magnetic separation, drug delivery, hyperthermia and MRI contrast enhancement, although these are only four of the many biomedical applications of magnetic nanoparticles that are currently being explored. For example, research is being conducted into magnetic twisting cytometry, a process in which ferromagnetic microspheres are bound to specific receptors on a cell wall. Changing the direction of an applied magnetic field twists the microsphere by a measurable amount, which can then be related to the mechanical properties of the cell membrane and cytoskeleton [139–143]. Magnetic nanoparticles are also being tested for tissue engineering applications, for example, in the mechanical conditioning of cells growing in culture [144–146]. In such systems magnetic particles are

attached to either the cell membrane, or to mechanosensitive ion channels in the membrane, and a magnetic force is applied which activates the channels and initiates biochemical reactions within the cell, thereby promoting the growth of e.g. functional bone and cartilage. A third example is magnetic biosensing: using magnetic nanoparticles coupled to analyte-specific molecules to detect target molecules via the crosslinking between coatings and the resultant aggregation of the magnetic particles, monitored by changes in proton relaxation times on a bench-top nuclear magnetic resonance system [147, 148].

One thing that almost all of these applications have in common, however, is that they are not yet market-based technologies. The exceptions are magnetic separation via cell and protein labelling, which is found in most biomedical and biochemistry laboratories today, and MRI contrast enhancement using encapsulated SPM nanoparticles, which is available (albeit not routinely used) in most hospital scanning facilities. Drug delivery via coating of nanoparticles is currently undergoing preliminary human trials, after successful tests in animals, with promising results, but it will be some time before it will be clinically available; and hyperthermia treatment of tumours is not yet accessible in humans, despite having been proven to be effective in animals. This highlights the fact that there is a significant step between a proven hypothetical process that has been tested under controlled laboratory conditions, and a close-to-market technology which can cope with the added complexity of in-service use. This is especially so if the goal is to transfer a procedure that has largely been the subject of *in vitro* or animal *in vivo* testing into a human *in vivo* therapy.

In short, one of the biggest challenges in biomedical applications of magnetic nanoparticles lies in dealing with the issue of technology transfer. There are opportunities in this respect for more interdisciplinary approaches, for example, to ensure that the laboratory based experiments can more explicitly emulate the expected conditions that would be encountered *in vivo*. There is also scope for significant contributions via the mathematical modelling of complex systems, with the objective of understanding more specifically the full gamut of physical phenomena and effects that together determine whether, in the final analysis, a given application will be successful.

References

- [1] Jiles D 1991 *Introduction to Magnetism and Magnetic Materials* (London: Chapman and Hall)
- [2] Morrish A H 2001 *The Physical Principles of Magnetism* (New York: IEEE Press)
- [3] Néel L 1949 *Ann. Geophys.* **5** 99–136
- [4] Brown W F Jr 1963 Thermal fluctuations of a single-domain particle *Phys. Rev.* **130** 1677–86
- [5] Gerber R 1994 Magnetic separation *Applied Magnetism* ed G Asti (Dordrecht: Kluwer) pp 165–220
- [6] Zborowski M 1997 Physics of magnetic cell sorting *Scientific and Clinical Applications of Magnetic Carriers* ed M Zborowski (New York: Plenum) pp 205–31
- [7] Hatch G P and Stelter R E 2001 Magnetic design considerations for devices and particles used for biological high-gradient magnetic separation (HGMS) systems *J. Magn. Magn. Mater.* **225** 262–76
- [8] Molday R S and MacKenzie D 1982 Immunospecific ferromagnetic iron–dextran reagents for the labeling and magnetic separation of cells *J. Immunol. Methods* **52** 353–67
- [9] Sangregorio C, Wiemann J K, O'Connor C J and Rosenzweig Z 1999 A new method for the synthesis of magnetoliposomes *J. Appl. Phys.* **85** 5699–701
- [10] Pardoe H, Chua-anusorn W, St Pierre T G and Dobson J 2001 Structural and magnetic properties of nanoscale iron oxide particles synthesized in the presence of dextran or polyvinyl alcohol *J. Magn. Magn. Mater.* **225** 41–6
- [11] Högemann D, Josephson L, Weissleder R and Basilion J P 2000 Improvement of MRI probes to allow efficient detection of gene expression *Bioconjugate Chem.* **11** 941–6
- [12] Levy L, Sahoo Y, Kim K S, Bergey E J and Prasad P N 2002 Nanochemistry: synthesis and characterization of multifunctional nanoclinics for biological applications *Chem. Mater.* **14** 3715–21
- [13] Zhang Y, Kohler N and Zhang M 2002 Surface modification of superparamagnetic magnetite nanoparticles and their intracellular uptake *Biomaterials* **23** 1553–61
- [14] Tibbe A, de Grooth B, Greve J, Liberti P, Dolan G and Terstappen L 1999 Optical tracking and detection of immunomagnetically selected and aligned cells *Nature Biotechnol.* **17** 1210–13
- [15] Kularatne B Y, Lorigan P, Browne S, Suvarna S K, Smith M O and Lawry J 2002 Monitoring tumour cells in the peripheral blood of small cell lung cancer patients *Cytometry* **50** 160–7
- [16] Morisada S, Miyata N and Iwahori K 2002 Immunomagnetic separation of scum-forming bacteria using polyclonal antibody that recognizes mycolic acids *J. Microbiol. Methods* **51** 141–8
- [17] Zigeuner R E, Riesenberger R, Pohla H, Hofstetter A and Oberneder R 2003 Isolation of circulating cancer cells from whole blood by immunomagnetic cell enrichment and unenriched immunocytochemistry *in vitro J. Urol.* **169** 701–5
- [18] Mura C V, Becker M I, Orellana A and Wolff D 2002 Immunopurification of Golgi vesicles by magnetic sorting *J. Immunol. Methods* **260** 263–71
- [19] Ugelstad J, Prestvik W S, Stenstad P, Kilaas L and Kvalheim G 1998 Selective cell separation with monosized magnetizable polymer beads *Magnetism in Medicine* ed H Nowak (Berlin: Wiley-VCH) pp 471–88
- [20] Hancock J P and Kemshead J T 1993 A rapid and highly selective approach to cell separations using an immunomagnetic colloid *J. Immunol. Methods* **164** 51–60
- [21] Owen C S 1983 Magnetic cell sorting *Cell Separation: Methods and Selected Applications* (New York: Academic)
- [22] Rheinländer T, Kötitz R, Weitschies W and Semmler W 2000 Magnetic fractionation of magnetic fluids *J. Magn. Magn. Mater.* **219** 219–28
- [23] Moore L, Rodeíguez A, Williams P, McCloskey B, Nakamura M, Chalmers J and Zborowski M 2001 Progenitor cell isolation with a high-capacity quadrupole magnetic flow sorter *J. Magn. Magn. Mater.* **225** 277–84
- [24] Rheinländer T, Roessner D, Weitschies W and Semmler W 1999 Comparison of size-selective techniques for the fractionation of magnetic nanospheres *Presented at Frontiers in Magnetism (Stockholm, Sweden)*
- [25] Todd P, Cooper R, Doyle J, Dunn S, Vellinger J and Deuser M 2001 Multistage magnetic particle separator *J. Magn. Magn. Mater.* **225** 294–300
- [26] Liberti P A, Rao C G and Terstappen L W M M 2001 Optimization of ferrofluids and protocols for the enrichment of breast tumor cells in blood *J. Magn. Magn. Mater.* **225** 301–7
- [27] Paul F, Melville D, Roath S and Warhurst D 1981 A bench top magnetic separator for malarial parasite concentration *IEEE Trans. Magn.* **MAG-17** 2822–4

- [28] Seesod N, Nopparat P, Hedrum A, Holder A, Thaithong S, Uhlen M and Lundeberg J 1997 An integrated system using immunomagnetic separation, polymerase chain reaction, and colorimetric detection for diagnosis of *Plasmodium Falciparum* *Am. J. Tropical Med. Hygiene* **56** 322–8
- [29] Hofmann W-K, de Vos S, Komor M, Hoelzer D, Wachsmann W and Koeffler H P 2002 Characterization of gene expression of CD34+ cells from normal and myelodysplastic bone marrow *Blood* **100** 3553–60
- [30] Delgratta C, Dellapenna S, Battista P, Didonato L, Vitullo P, Romani G and Diluzio S 1995 Detection and counting of specific cell populations by means of magnetic markers linked to monoclonal antibodies *Phys. Med. Biol.* **40** 671–81
- [31] Edelstein R L, Tamanaha C R, Sheehan P E, Miller M M, Baselt D R, Whitman L J and Colton R J 2000 The BARC biosensor applied to the detection of biological warfare agents *Biosensors Bioelectron.* **14** 805–13
- [32] Kala M, Bajaj K and Sinha S 1997 Magnetic bead enzyme-linked immunosorbent assay (ELISA) detects antigen-specific binding by phage-displayed scFv antibodies that are not detected with conventional ELISA *Anal. Biochem.* **254** 263–6
- [33] Yazdankhah S P, Hellemann A-L, Ronningen K and Olsen E 1998 Rapid and sensitive detection of *Staphylococcus* species in milk by ELISA based on monodisperse magnetic particles *Veterinary Microbiol.* **62** 17–26
- [34] Widder K J, Senyei A E and Scarpelli D G 1978 Magnetic microspheres: a model system for site specific drug delivery *in vivo Proc. Soc. Exp. Biol. Med.* **58** 141–6
- [35] Senyei A, Widder K and Czerlinski C 1978 Magnetic guidance of drug carrying microspheres *J. Appl. Phys.* **49** 3578–83
- [36] Mosbach K and Schröder U 1979 Preparation and application of magnetic polymers for targeting of drugs *FEBS Lett.* **102** 112–6
- [37] Alexiou C, Arnold W, Klein R J, Parak F G, Hulin P, Bergemann C, Erhardt W, Wagenpfeil S and Lubbe A S 2000 Locoregional cancer treatment with magnetic drug targeting *Cancer Res.* **60** 6641–8
- [38] Lübke A S, Bergemann C, Brock J and McClure D G 1999 Physiological aspects in magnetic drug-targeting *J. Magn. Magn. Mater.* **194** 149–55
- [39] Voltairas P A, Fotiadis D I and Michalis L K 2002 Hydrodynamics of magnetic drug targeting *J. Biomech.* **35** 813–21
- [40] Cummings L J, Richardson G and Hazelwood L 2000 Drug delivery by magnetic microspheres *Proc. Mathematics in Medicine Study Group* (Nottingham, UK: University of Nottingham) pp 69–83
- [41] Dobson J, Gross B, Exley C, Mickhailova A, Batich C and Pardoe H 2001 Biomedical applications of biogenic and biocompatible magnetic nanoparticles *Modern Problems of Cellular and Molecular Biophysics* ed S Ayrapetyan and A North (Yerevan: Noyan Tapan/UNESCO) pp 121–30
- [42] Mehta R V, Upadhyay R V, Charles S W and Ramchand C N 1997 Direct binding of protein to magnetic particles *Biotechnol. Techn.* **11** 493–6
- [43] Koneracka M, Kopcansky P, Antalk M, Timko M, Ramchand C N, Lobo D, Mehta R V and Upadhyay R V 1999 Immobilization of proteins and enzymes to fine magnetic particles *J. Magn. Magn. Mater.* **201** 427–30
- [44] Koneracka M, Kopcansky P, Timko M, Ramchand C N, de Sequeira A and Trevan M 2002 Direct binding procedure of proteins and enzymes to fine magnetic particles *J. Mol. Catalysis B Enzymatic* **18** 13–8
- [45] Hans M L and Lowman A M 2002 Biodegradable nanoparticles for drug delivery and targeting *Curr. Opin. Solid State Mater. Sci.* **6** 319–27
- [46] Grüttner C and Teller J 1999 New types of silica-fortified magnetic nanoparticles as tools for molecular biology applications *J. Magn. Magn. Mater.* **194** 8–15
- [47] Rudge S R, Kurtz T L, Vessely C R, Catterall L G and Williamson D L 2000 Preparation, characterization, and performance of magnetic iron–carbon composite microparticles for chemotherapy *Biomaterials* **21** 1411–20
- [48] Arias J L, Gallardo V, Gomez-Lopera S A, Plaza R C and Delgado A V 2001 Synthesis and characterization of poly(ethyl-2-cyanoacrylate) nanoparticles with a magnetic core *J. Control. Release* **77** 309–21
- [49] Gomez-Lopera S A, Plaza R C and Delgado A V 2001 Synthesis and characterization of spherical magnetite/biodegradable polymer composite particles *J. Colloid Interface Sci.* **240** 40–7
- [50] Mornet S, Grasset F, Portier J and D E 2002 Maghemite/silica nanoparticles for biological applications *Eur. Cells Mater.* **3** 110–3
- [51] Deng Y, Wang L, Yang W, Fu S and Elaissari A 2003 Preparation of magnetic polymeric particles via inverse microemulsion polymerization process *J. Magn. Magn. Mater.* **257** 69–78
- [52] Santra S, Tapeç R, Theodoropoulou N, Dobson J, Hebard A and Tan W 2001 Synthesis and characterization of silica-coated iron oxide nanoparticles in microemulsion: the effect of nonionic surfactants *Langmuir* **17** 2900–6
- [53] Carpenter E E 2001 Iron nanoparticles as potential magnetic carriers *J. Magn. Magn. Mater.* **225** 17–20
- [54] Stevenson J P, Rutnakornpituk M, Vadala M, Esker A R, Charles S W, Wells S, Dailey J P and Riffle J S 2001 Magnetic cobalt dispersions in poly(dimethylsiloxane) fluids *J. Magn. Magn. Mater.* **225** 47–58
- [55] Connolly J, St Pierre T G, Rutnakornpituk M and Riffle J S 2002 Silica coating of cobalt nanoparticles increases their magnetic and chemical stability for biomedical applications *Eur. Cells Mater.* **3** 106–9
- [56] Sun X, Gutierrez A, Yacaman M J, Dong X and Jin S 2000 Investigations on magnetic properties and structure for carbon encapsulated nanoparticles of Fe, Co, Ni *Mater. Sci. Eng.* **286** 157–60
- [57] Grasset F, Mornet S, Demourgues A, Portier J, Bonnet J, Vekris A and Duguet E 2001 Synthesis, magnetic properties, surface modification and cytotoxicity evaluation of $Y_3Fe_{5-x}Al_xO_{12}$ garnet submicron particles for biomedical applications *J. Magn. Magn. Mater.* **234** 409–18
- [58] Dailey J P, Phillips J P, Li C and Riffle J S 1999 Synthesis of silicone magnetic fluid for use in eye surgery *J. Magn. Magn. Mater.* **194** 140–8
- [59] Rutnakornpituk M, Baranauskas V, Riffle J S, Connolly J, St Pierre T G and Dailey J P 2002 Polysiloxane fluid dispersions of cobalt nanoparticles in silica spheres for use in ophthalmic applications *Eur. Cells Mater.* **3** 102–5
- [60] Widder K J, Morris R M, Poore G A, Howard D P and Senyei A E 1983 Selective targeting of magnetic albumin microspheres containing low-dose doxorubicin—total remission in Yoshida sarcoma-bearing rats *Eur. J. Cancer Clin. Oncol.* **19** 135–9
- [61] Goodwin S, Peterson C, Hob C and Bittner C 1999 Targeting and retention of magnetic targeted carriers (MTCs) enhancing intra-arterial chemotherapy *J. Magn. Magn. Mater.* **194** 132–9
- [62] Goodwin S C, Bittner C A, Peterson C L and Wong G 2001 Single-dose toxicity study of hepatic intra-arterial infusion of doxorubicin coupled to a novel magnetically targeted drug carrier *Toxicol. Sci.* **60** 177–83
- [63] Pulfer S K and Gallo J M 1999 Enhanced brain tumor selectivity of cationic magnetic polysaccharide microspheres *J. Drug Targeting* **6** 215–28
- [64] Pulfer S K, Ciccotto S L and Gallo J M 1999 Distribution of small magnetic particles in brain tumor-bearing rats *J. Neuro-Oncol.* **41** 99–105

- [65] Kubo T, Sugita T, Shimose S, Nitta Y, Ikuta Y and Murakami T 2000 Targeted delivery of anticancer drugs with intravenously administered magnetic liposomes in osteosarcoma-bearing hamsters *Int. J. Oncol.* **17** 309–16
- [66] Kubo T, Sugita T, Shimose S, Nitta Y, Ikuta Y and Murakami T 2001 Targeted systemic chemotherapy using magnetic liposomes with incorporated adriamycin for osteosarcoma in hamsters *Int. J. Oncol.* **18** 121–6
- [67] Mykhaylyk O, Cherchenko A, Ilkin A, Dudchenko N, Ruditsa V, Novoseletz M and Zozulya Y 2001 Glial brain tumor targeting of magnetite nanoparticles in rats *J. Magn. Magn. Mater.* **225** 241–7
- [68] Lübke A S, Bergemann C, Huhnt W, Fricke T, Riess H, Brock J W and Huhn D 1996 Preclinical experiences with magnetic drug targeting: tolerance and efficacy *Cancer Res.* **56** 4694–701
- [69] Lübke A S, Bergemann C, Riess H, Schriever F, Reichardt P, Possinger K, Matthias M, Doerken B, Herrmann F and Guertler R 1996 Clinical experiences with magnetic drug targeting: a phase I study with 4'-epidoxorubicin in 14 patients with advanced solid tumors *Cancer Res.* **56** 4686–93
- [70] Lübke A S and Bergemann C 1996 Selected preclinical and first clinical experiences with magnetically targeted 4'-epidoxorubicin in patients with advanced solid tumors Presented at *International Conf. on Scientific and Clinical Applications of Magnetic Carriers (Rostock, Germany)*
- [71] Häfeli U O and Pauer G J 1999 *In vitro* and *in vivo* toxicity of magnetic microspheres *J. Magn. Magn. Mater.* **194** 76–82
- [72] Gallo J M and Häfeli U 1997 Preclinical experiences with magnetic drug targeting: tolerance and efficacy and clinical experiences with magnetic drug targeting: a phase I study with 4'-epidoxorubicin in 14 patients with advanced solid tumors *Cancer Res.* **57** 3063–4
- [73] Häfeli U O, Sweeney S M, Beresford B A and Humm J L 1995 Effective targeting of magnetic radioactive ⁹⁰Y-microspheres to tumor cells by an externally applied magnetic field. Preliminary *in vitro* and *in vivo* results *Nucl. Med. Biol.* **22** 147
- [74] Häfeli U O, Pauer G J, Roberts W K and Humm J L 1996 Magnetically targeted microspheres for intracavitary and intraspinal Y-90 radiotherapy Presented at *International Conf. on Scientific and Clinical Applications of Magnetic Carriers (Rostock, Germany)*
- [75] Häfeli U O, Casillas S, Dietz D W, Pauer G J, Rybicki L A, Conzone S D and Day D E 1999 Hepatic tumor radioembolization in a rat model using radioactive rhenium (¹⁸⁶Re/¹⁸⁸Re) glass microspheres *Int. J. Radiat. Oncol. Biol. Phys.* **44** 189–200
- [76] Häfeli U, Pauer G, Failing S and Tapolsky G 2001 Radiolabeling of magnetic particles with rhenium-188 for cancer therapy *J. Magn. Magn. Mater.* **225** 73–8
- [77] Mah C, Zolotukhin I, Fraites T J, Dobson J, Batich C and Byrne B J 2000 Microsphere-mediated delivery of recombinant AAV vectors *in vitro* and *in vivo* *Mol. Therapy* **1** S239
- [78] Mah C, Fraites T J, Zolotukhin I, Song S, Flotte T R, Dobson J, Batich C and Byrne B J 2002 Improved method of recombinant AAV2 delivery for systemic targeted gene therapy *Mol. Therapy* **6** 106–12
- [79] Hughes C, Galea-Lauri J, Farzaneh F and Darling D 2001 Streptavidin paramagnetic particles provide a choice of three affinity-based capture and magnetic concentration strategies for retroviral vectors *Mol. Therapy* **3** 623–30
- [80] Van der Zee J 2002 Heating the patient: a promising approach? *Ann. Oncol.* **13** 1173–84
- [81] Wust P, Hildebrandt B, Sreenivasa G, Rau B, Gellermann J, Riess H, Felix R and Schlag P M 2002 Hyperthermia in combined treatment of cancer *Lancet Oncol.* **3** 487–97
- [82] Moroz P, Jones S K and Gray B N 2001 Status of hyperthermia in the treatment of advanced liver cancer *J. Surg. Oncol.* **77** 259–69
- [83] Gilchrist R K, Medal R, Shorey W D, Hanselman R C, Parrott J C and Taylor C B 1957 Selective inductive heating of lymph nodes *Ann. Surg.* **146** 596–606
- [84] Mosso J A and Rand R W 1972 Ferromagnetic silicone vascular occlusion *Ann. Surg.* 663–8
- [85] Rand R W, Snyder M, Elliott D G and Snow H D 1976 Selective radiofrequency heating of ferrosilicone occluded tissue: a preliminary report *Bull. Los Angeles Neurol. Soc.* **41** 154–9
- [86] Gordon R T, Hines J R and Gordon D 1979 Intracellular hyperthermia: a biophysical approach to cancer treatment via intracellular temperature and biophysical alterations *Med. Hypotheses* **5** 83–102
- [87] Rand R W, Snow H D, Elliott D G and Snyder M 1981 Thermomagnetic surgery for cancer *Appl. Biochem. Biotechnol.* **6** 265–72
- [88] Borrelli N F, Luderer A A and Panzarino J N 1984 Hysteresis heating for the treatment of tumours *Phys. Med. Biol.* **29** 487–94
- [89] Hase M, Sako M and Hirota S 1990 Experimental study of ferromagnetic induction heating combined with hepatic arterial embolization of liver tumours *Nippon-Igaku-Hoshasen-Gakkai-Zasshi* **50** 1402–14
- [90] Suzuki S, Arai K, Koike T and Oguchi K 1990 Studies on liposomal ferromagnetic particles and a technique of high frequency inductive heating—*in vivo* studies of rabbits *J. Japan. Soc. Cancer Therapy* **25** 2649–58
- [91] Chan D C F, Kirpotin D B and Bunn P A Jr 1993 Synthesis and evaluation of colloidal magnetic iron oxides for the site-specific radiofrequency-induced hyperthermia of cancer *J. Magn. Magn. Mater.* **122** 374–8
- [92] Matsuki H, Yanada T, Sato T, Murakami K and Minakawa S 1994 Temperature sensitive amorphous magnetic flakes for intratissue hyperthermia *Mater. Sci. Eng.* **A181/A182** 1366–8
- [93] Mitsumori M *et al* 1994 Development of intra-arterial hyperthermia using a dextran-magnetite complex *Int. J. Hyperthermia* **10** 785–93
- [94] Suzuki M, Shinkai M, Kamihira M and Kobayashi T 1995 Preparation and characteristics of magnetite-labelled antibody with the use of poly(ethylene glycol) derivatives *Biotechnol. Appl. Biochem.* **21** 335–45
- [95] Mitsumori M, Hiraoka M, Shibata T, Okuno Y, Nagata Y, Nishimura Y, Abe M, Hasegawa M, Nagae H and Ebisawa Y 1996 Targeted hyperthermia using dextran magnetite complex: a new treatment modality for liver tumours *Hepato-Gastroenterology* **43** 1431–7
- [96] Jordan A, Scholz R, Wust P, Fahling H, Krause J, Wlodarczyk W, Sander B, Vogl T and Felix R 1997 Effects of magnetic fluid hyperthermia (MFH) on C₃H mammary carcinoma *in vivo* *Int. J. Hyperthermia* **13** 587–605
- [97] Shinkai M, Yanase M, Suzuki M, Honda H, Wakabayashi T, Yoshida J and Kobayashi T 1999 Intracellular hyperthermia for cancer using magnetite cationic liposomes *J. Magn. Magn. Mater.* **194** 176–84
- [98] Jordan A, Scholz R, Wust P, Fahling H and Felix R 1999 Magnetic fluid hyperthermia (MFH): cancer treatment with AC magnetic field induced excitation of biocompatible superparamagnetic nanoparticles *J. Magn. Magn. Mater.* **201** 413–19
- [99] Minamimura T, Sato H, Kasaoka S, Saito T, Ishizawa S, Takemori S, Tazawa K and Tsukada K 2000 Tumour regression by inductive hyperthermia combined with hepatic embolization using dextran magnetite incorporated microspheres in rats *Int. J. Oncol.* **16** 1153–8
- [100] Moroz P, Jones S K, Winter J and Gray B N 2001 Targeting liver tumors with hyperthermia: ferromagnetic embolization in a rabbit liver tumor model *J. Surg. Oncol.* **78** 22–9
- [101] Jones S K, Winter J W and Gray B N 2002 Treatment of experimental rabbit liver tumours by selectively targeted hyperthermia *Int. J. Hyperthermia* **18** 117–28

- [102] Hilger I, Fruhauf K, Andra W, Hiergeist R, Hergt R and Kaiser W A 2002 Heating potential of iron oxides for therapeutic purposes in interventional radiology *Acad. Radiol.* **9** 198–202
- [103] Moroz P, Jones S K and Gray B N 2002 Magnetically mediated hyperthermia: current status and future directions *Int. J. Hyperthermia* **18** 267–84
- [104] Rabin Y 2001 Is intracellular hyperthermia superior to extracellular hyperthermia in the thermal sense? *Int. J. Hyperthermia*
- [105] Granov A M, Muratov O V and Frolov V F 2002 Problems in the local hyperthermia of inductively heated embolized tissues *Theor. Foundations Chem. Eng.* **36** 63–6
- [106] Craciun V, Calugaru G and Badescu V 2002 Accelerated simulation of heat transfer in magnetic fluid hyperthermia *Czechoslovak J. Phys.* **52** 725–8
- [107] Oleson J R, Cetas T C and Corry P M 1983 Hyperthermia by magnetic induction: experimental and theoretical results for coaxial coil pairs *Radiat. Res.* **95** 175–86
- [108] Reilly J P 1992 Principles of nerve and heart excitation by time-varying magnetic fields *Ann. New York Acad. Sci.* **649** 96–117
- [109] Oleson J R, Heusinkveld R S and Manning M R 1983 Hyperthermia by magnetic induction: II. Clinical experience with concentric electrodes *Int. J. Radiat. Oncol. Biol. Phys.* **9** 549–56
- [110] Atkinson W J, Brezovich I A and Chakraborty D P 1984 Usable frequencies in hyperthermia with thermal seeds *IEEE Trans. Biomed. Eng.* **BME 31** 70–5
- [111] Jordan A, Wust P, Fahling H, Johns W, Hinz A and Felix R 1993 Inductive heating of ferrimagnetic particles and magnetic fluids: physical evaluation of their potential for hyperthermia *Int. J. Hyperthermia* **9** 51–68
- [112] Jordan A *et al* 2001 Presentation of a new magnetic field therapy system for the treatment of human solid tumours with magnetic fluid hyperthermia *J. Magn. Magn. Mater.* **225** 118–26
- [113] Rosensweig R E 2002 Heating magnetic fluid with alternating magnetic field *J. Magn. Magn. Mater.* **252** 370–4
- [114] Debye P 1929 *Polar Molecules* (New York: The Chemical Catalog Company)
- [115] Fannin P C and Charles S W 1991 Measurement of the Neel relaxation of magnetic particles in the frequency range 1 kHz–160 MHz *J. Phys. D: Appl. Phys.* **24** 76–7
- [116] Fannin P C, Scaife B K P and Charles S W 1993 Relaxation and resonance in ferrofluids *J. Magn. Magn. Mater.* **122** 159–63
- [117] Hanson M 1991 The frequency dependence of the complex susceptibility of magnetic liquids *J. Magn. Magn. Mater.* **96** 105–13
- [118] Jones S K, Gray B N, Burton M A, Codde J P and Street R 1992 Evaluation of ferromagnetic materials for low frequency hysteresis heating of tumours *Phys. Med. Biol.* **37** 293–9
- [119] Maehara T, Konishi K, Kamimori T, Aono H, Naohara T, Kikkawa H, Watanabe Y and Kawachi K 2002 Heating of ferrite powder by an AC magnetic field for local hyperthermia *Japan. J. Appl. Phys.* **41** 1620–1
- [120] Kirpotin D, Chan D C F and Bunn P A 1995 Magnetic microparticles *US Patents* vol 5,411,730 (Tucson, AZ) (USA: Research Corporation Technologies, Inc.)
- [121] Hergt R, Andra W, d'Ambly C, Hilger I, Kaiser W, Richter U and Schmidt H 1998 Physical limits of hyperthermia using magnetite fine particles *IEEE Trans. Magn.* **34** 3745–54
- [122] Livingston J D 1996 *Driving Force: The Natural Magic of Magnets* (Cambridge: Harvard University Press)
- [123] Elster A and Burdette J 2001 *Questions and Answers in Magnetic Resonance Imaging* (St Louis, USA: Mosby)
- [124] Leach M O 1988 Spatially localised nuclear magnetic resonance *The Physics of Medical Imaging* ed S Webb (Bristol, UK: Adam Hilger) pp 389–487
- [125] Browne M and Semelka R C 1999 *MRI: Basic Principles and Applications* (New York: Wiley)
- [126] Lawaczeck R, Bauer H, Frenzel T, Hasegawa M, Ito Y, Kito K, Miwa N, Tsutsui H, Vogler H and Weinmann H J 1997 Magnetic iron oxide particles coated with carboxydextran for parenteral administration and liver contrasting *Acta Radiol.* **38** 584–97
- [127] Weissleder R, Elizondo G, Wittenburg J, Rabito C A, Bengele H H and Josephson L 1990 Ultrasmall superparamagnetic iron oxide: characterization of a new class of contrast agents for MR imaging *Radiol.* **175** 489–93
- [128] Ruehm S G, Corot C, Vogt P, Kolb S and Debatin J F 2001 Magnetic resonance imaging of atherosclerotic plaque with ultrasmall superparamagnetic particles of iron oxide in hyperlipidemic rabbits *Circulation* **103** 415–22
- [129] Wacker F K, Reither K, Ebert W, Wendt M, Lewin J S and Wolf K J 2003 MR image-guided endovascular procedures with the ultrasmall superparamagnetic iron oxide SHU555C as an intravascular contrast agent: study in pigs *Radiology* **226** 459–64
- [130] Dosset V, Gomez C, Petry K G, Delalande C and Caille J-M 1999 Dose and scanning delay using USPIO for central nervous system macrophage imaging *Magn. Res. Mater. Phys., Biol. Med.* **8** 185–9
- [131] Michel S C A, Keller T M, Frohlich J M, Fink D, Caduff R, Seifert B, Marincek B and Kubik-Huch R A 2002 Preoperative breast cancer staging: MR imaging of the axilla with ultrasmall superparamagnetic iron oxide enhancement *Radiology* **225** 527–36
- [132] Semelka R C and Helmberger T K G 2001 Contrast agents for MR imaging of the liver *Radiology* **218** 27–38
- [133] Enochs W S, Harsh G, Hochberg F and Weissleder R 1999 Improved delineation of human brain tumours on MR images using a long-circulating, superparamagnetic iron oxide agent *J. Magn. Res. Imag.* **9** 228–32
- [134] Bulte J, de Cuyper M, Despres D and Frank J 1999 Short- vs long-circulating magnetoliposomes as bone marrow-seeking MR contrast agents *J. Magn. Res. Imag.* **9** 329–35
- [135] Bulte J *et al* 2001 Magnetodendrimers allow endosomal magnetic labeling and *in vivo* tracking of stem cells *Nature Biotechnol.* **19** 1141–7
- [136] Hoehn M *et al* 2002 Monitoring of implanted stem cell migration *in vivo*: a highly resolved *in vivo* magnetic resonance imaging investigation of experimental stroke in rat *Proc. Natl Acad. Sci. USA* **99** 16267–72
- [137] Weissleder R, Moore A, Mahmood U, Bhorade R, Benveniste H, Chiocca E A and Basilion J P 2000 *In vivo* magnetic resonance imaging of transgene expression *Nature Med.* **6** 351–4
- [138] Zhao M, Beauregard D, Loizou L, Davletov B and Brindle K 2001 Non-invasive detection of apoptosis using magnetic resonance imaging and a targeted contrast agent *Nature Med.* **7** 1241–4
- [139] Wang N, Butler J P and Ingber D E 1993 Mechanotransduction across the cell surface and through the cytoskeleton *Science* **260** 1124
- [140] Fabry B, Maksym G N, Hubmayr R D, Butler J P and Fredberg J J 1999 Implications of heterogeneous bead behavior on cell mechanical properties measured with magnetic twisting cytometry *J. Magn. Magn. Mater.* **194** 120–5
- [141] Fabry B, Maksym G N, Butler J P, Glogauer M, Navajas D and Fredberg J J 2001 Scaling the microrheology of living cells *Phys. Rev. Lett.* **87** 148102
- [142] Bausch A R, Ziemann F, Boulbitch A A, Jacobson K and Sackmann E 1998 Local measurements of viscoelastic

- parameters of adherent cell surfaces by magnetic bead microrheometry *Biophys. J.* **75** 2038–49
- [143] Bausch A R, Moeller W and Sackmann E 1999 Measurement of local viscoelasticity and forces in living cells by magnetic tweezers *Biophys. J.* **76** 573–9
- [144] Dobson J, Keramane A and El Haj A J 2002 Theory and applications of a magnetic force bioreactor *Eur. Cells Mater.* **4** 130–1
- [145] Cartmell S H, Dobson J, Verschuereen S, Hughes S and El Haj A J 2002 Mechanical conditioning of bone cells *in vitro* using magnetic microparticle technology *Eur. Cells Mater.* **4** 42–4
- [146] Cartmell S H, Dobson J, Verschuereen S and El Haj A J 2003 Preliminary analysis of magnetic particle techniques for activating mechanotransduction in bone cells *IEEE Trans. NanoBiosci.* at press
- [147] Perez J M, Josephson L, O Loughlin T, Hogemann D and Weissleder R 2002 Magnetic relaxation switches capable of sensing molecular interactions *Nature Biotechnol.* **20** 816–20
- [148] Perez J M, O Loughlin T, Simeone F J, Weissleder R and Josephson L 2002 DNA-based magnetic nanoparticle assembly acts as a magnetic relaxation nanoswitch allowing screening of DNA-cleaving agents *J. Am. Chem. Soc.* **124** 2856–7